Published in final edited form as:
Neuroimage. 2012 March ; 60(1): 263–270. doi:10.1016/j.neuroimage.2011.11.070.

Myelin Water Imaging Reflects Clinical Variability in Multiple Sclerosis

Shannon Kolind[a,b], **Lucy Matthews**[a,c], **Heidi Johansen-Berg**[a], **M Isabel Leite**[c], **Steven C R Williams**[b], **Sean Deoni**[b,d], and **Jackie Palace**[c]

[a]FMRIB Centre, Nuffield Department of Clinical Neurosciences, University of Oxford, UK

[b]Department of Neuroimaging, Institute of Psychiatry, King's College London, London, UK

[c]Department of Clinical Neurology, Oxford University and Oxford Radcliffe Hospitals NHS Trust, UK

[d]School of Engineering, Brown University, Providence, Rhode Island, USA

Abstract

Whilst MRI is routinely used for the assessment and diagnosis of multiple sclerosis, there is poor correspondence between clinical disability in primary progressive multiple sclerosis (PPMS) patients and conventional MRI markers of disease activity (e.g., number of enhancing lesions). As PPMS patients show diffuse and global myelin loss, the aim of this study was to evaluate the efficacy of whole-brain myelin water fraction (MWF) imaging in PPMS. Specifically, we sought to use full-brain analysis techniques to: 1) determine the reproducibility of MWF estimates in PPMS brain; 2) compare MWF values in PPMS brain to healthy controls; and 3) establish the relationship between MWF and clinical disability, regionally and globally throughout the brain. Seventeen PPMS patients and seventeen age-matched controls were imaged using a whole-brain multi-component relaxation imaging technique to measure MWF. Analysis of MWF reduction was performed on three spatial levels: 1) histogram; 2) white matter skeleton; and 3) voxel-wise at the single-subject level. From histogram analysis, PPMS patients had significantly reduced global normal appearing white matter MWF (6%, $p=0.04$) compared to controls. Focal lesions showed lower MWF values than white matter in controls (61%, $p<0.001$) and patients (59%, $p<0.001$). Along the white matter skeleton, MWF was diffusely reduced throughout the PPMS brain, with significant correlations between reduced MWF and increased clinical disability (more severe symptoms), as measured by the Expanded Disability Status Scale, within the corpus callosum and frontal, temporal, parietal and occipital white matter. Correlations with the more specific mental and sensory functional system scores were localized to clinically eloquent locations: reduced MWF was significantly associated with increased mental scores in anterior regions (i.e., frontal lobes and genu of the corpus callosum), and increased sensory scores in more posterior regions closer to the sensory cortex. Individual patient MWF maps were also compared to a normative population atlas, which highlighted areas of statistical difference between the individual patient and the population mean. A significant correlation was found between the volume of significantly reduced MWF and clinical disability ($p=0.008$, $R = 0.58$). Our results show that clinical disability is reflected in particular regions of cerebral white matter that are consistent between subjects, and illustrates a method to examine tissue alteration throughout the brain of individual patients. These results strongly support the use of MWF imaging to evaluate disease activity in PPMS.

Please address correspondence to: Shannon H. Kolind FMRIB Centre University of Oxford Department of Clinical Neurology John Radcliffe Hospital Headington Oxford, UK OX3 9DU Telephone: +44 (0)1865 222729 Fax: +44 (0)1865 222717 skolind@fmrib.ox.ac.uk.

Europe PMC Funders Author Manuscripts

Keywords

multiple sclerosis (MS); magnetic resonance imaging (MRI); brain; myelin water imaging; multi-component relaxation

1. INTRODUCTION

Of the four primary multiple sclerosis (MS) sub-types, primary progressive MS (PPMS) is clinically differentiated by a constant progression of disability, devoid of intermittent relapses or periods of remission (Miller and Leary, 2007). Despite the more disabling nature of this disease phenotype compared to the more common relapsing remitting MS, it is associated with fewer T_2-hyperintense, T1-hypotintense and gadolinium-enhancing lesions on magnetic resonance images (Miller and Leary, 2007). Histologically, PPMS lesions differ in both number and underlying pathology, with PPMS demyelinated lesions containing fewer inflammatory cells (Revesz et al., 1994); less acute axonal damage (Bitsch et al., 2000); and extensive remyelination in a large proportion of the lesion area in a subset of PPMS patients (Patrikios et al., 2006). Conventional magnetic resonance imaging (MRI) is unable to delineate the underlying cause or composition of lesions, which may represent areas of inflammation, demyelination, myelin repair, axonal loss or scar tissue. Irrespective of the underlying pathology, however, the extent of visible damage in the brain does not correspond well to symptoms (Rocca et al., 2011). Further, as most current MR-based metrics (such as number of enhancing lesions) of MS disease activity are based on focal brain inflammation, they are less suited to assess disease activity in PPMS.

Histological studies of PPMS brain specimens have shown extensive cortical demyelination and diffuse damage with myelin loss and axonal injury even in the non-lesional normal-appearing white and grey matter tissue (Kutzelnigg et al., 2005). Unfortunately, conventional T_1 or T_2-*weighted* MRI is non-specific to these pathological effects and these abnormalities are not readily discernible on current standard imaging. *Quantitative* MRI, in contrast, may be more sensitive to inconspicuous tissue injury. T_1 or T_2-relaxation measurement (Grenier et al., 2002; Manfredonia et al., 2007), magnetization transfer imaging (MTI) (Khaleeli et al., 2007; Miller et al., 2003; Rabe-Jabloska, 2003), diffusion tensor imaging (DTI) (Ceccarelli et al., 2009; Rovaris et al., 2006; Schmierer et al., 2004), atrophy measurements (Sastre-Garriga et al., 2005a), and proton MR spectroscopy (MRS) (Rovaris et al., 2002; Sastre-Garriga et al., 2005b) have all revealed abnormalities in normal-appearing brain tissue not visible on standard T_1 or T_2-*weighted* images. Further, these measures have shown greater correspondence to clinical disability and progression than measures relating to focal lesions.

While quantitative MRI demonstrates the potential for investigating disease pathology *in vivo*, it is also important to differentiate between contributing pathological processes, including inflammation, axonal damage, and particularly, myelin damage, as these may distinguish between different MS subtypes and provide a greater understanding of disease pathogenesis and treatment effect. While sensitive to these diverse effects, individual quantitative MRI metrics are non-specific and are influenced nonlinearly by the tissue microstructure and biochemistry. For example, MTI provides estimates of macromolecular-bound water, assumed to be associated with myelin, but macromolecules are not restricted to myelin, and the bound water fraction estimate is also strongly influenced by inflammation (Gareau et al., 2000; Vavasour et al., 2011; Vavasour et al., 1998). DTI, while exquisitely sensitive to the microstructural architecture, reflects not only myelin, but also fibre coherence, axonal density, and membrane permeability (Beaulieu, 2002; Harsan et al., 2006).

Europe PMC Funders Author Manuscripts

In this study we sought to apply a more myelin-specific quantitative MRI technique, multi-component relaxation analysis, to investigate diffuse myelin alterations associated with PPMS. Multi-component relaxation aims to separate the measured MRI signal into contributions from sub-voxel anatomical water pools. In central nervous system tissue, these water pools broadly correspond to intra- and extra-cellular water, which relaxes slowly, and water trapped between the myelin bilayers, which relaxes more quickly. The myelin-associated water volume fraction, termed the myelin water fraction (MWF), has been shown to correlate strongly with gold-standard histopathological measurements of myelin content (Kozlowski et al., 2008; Laule et al., 2008; Laule et al., 2006a; Moore et al., 2000; Odrobina et al., 2005; Pun et al., 2005; Stanisz et al., 2004; Stewart et al., 1993; Webb et al., 2003), thus providing a non-invasive surrogate measure of myelin content.

Though the application of multi-component relaxation imaging in MS is not new, previous studies have typically employed a single-slice technique (Kolind et al., 2008; Laule et al., 2007; Laule et al., 2011; Laule et al., 2004; Vavasour et al., 2007), limiting the investigation of global diffuse tissue damage and hindering interpretation and generalisation of results. The technique we chose, mcDESPOT (multi-component Driven Equilibrium Single Pulse Observation of T1 & T2) (Deoni et al., 2008), provides full volumetric brain coverage with high resolution, allowing more thorough characterization of the diffuse myelin changes expected to be present in PPMS, and their relation to clinical severity. Here, we aimed to determine the suitability of MWF as a biomarker for PPMS. Specifically, we sought to use full-brain analysis techniques to: 1) determine the reproducibility of mcDESPOT-derived myelin content estimates in PPMS brain; 2) compare MWF values in PPMS brain to healthy controls; and 3) establish the relationship between MWF and clinical disability, regionally and globally throughout the brain.

2. MATERIALS AND METHODS

2.1. *Subjects*

Seventeen subjects with clinically definite PPMS fulfilling the 2005 revised MacDonald's criteria for diagnosis (Polman et al., 2005) [11 female, 6 male; mean age = 51 years (range: 35 – 60 years); mean disease duration = 9 years (range 4 – 19 years)] and 17 healthy volunteers without neurological disease, age-matched to the PPMS cohort [9 female, 8 male; mean age = 50 years (range: 32 – 64 years)] were included in the study.

All patients underwent a full neurological examination and evaluation of the Kurtzke Expanded Disability Status Scale (EDSS) (Kurtzke, 1983) [median EDSS = 5.5 (range: 1.5-6.5)], which included evaluation of the functional system (FS) scores involved in the determination of the EDSS (pyramidal, cerebellar, brainstem, sensory, bowel & bladder, visual, and mental).

Nine of the PPMS patients and 7 of the healthy controls underwent a second MRI scan within a 2-week interval to investigate measurement reproducibility.

The study was approved by the local Ethical Committee and written informed consent was obtained from all participants.

2.2. *MRI Data Acquisition*

All MR imaging was performed on a Siemens Avanto 1.5T scanner using an 8-channel head radio-frequency array coil.

The mcDESPOT protocol was comprised of series of sagittally-oriented spoiled gradient recalled echo (SPGR) and balanced steady state free procession (bSSFP) acquisitions across

a range of flip angles (α). A common field of view of 22 × 22 × 18 cm and voxel size of 1.7 × 1.7 × 1.7 mm was used. Other scan parameters were: SPGR: TE = 2.5 ms; TR = 6.0 ms; BW = 350 Hz/pixel; α = [3, 4, 5, 6, 7, 9, 12, 18]°. bSSFP: TE = 1.9 ms; TR = 3.8 ms; BW = 930 Hz/pixel; α = [10, 14, 21, 28, 34, 41, 51, 68]°; all flip angles were acquired with phase-cycling patterns of ϕ = 0° and 180° for correction of off-resonance effects (Deoni, 2011). Total mcDESPOT acquisition time was under 14 minutes.

In addition to mcDESPOT, conventional clinical anatomical images were also acquired. These included proton density and T_2-*weighted* images (dual-echo turbo spin echo sequence, $TE_1/TE_2/TR$ = 22/88/3000 ms, field of view = 25 × 25 × 15 cm, voxel size of 1 × 1 × 3 mm, α = 150°) acquired in a transverse plane parallel to the line connecting the anterior commissure to the posterior commissure for lesion identification. A high-resolution sagittal T_1-weighted volume (MP-RAGE sequence, TE = 5ms, TR = 2600ms, field of view = 25 × 22 × 18 cm, voxel size of 1 × 1 × 1.2 mm, α = 10°) was acquired for registration and segmentation of white matter (WM) and grey matter (GM).

2.3. Data Analysis

2.3.1. mcDESPOT Analysis—mcDESPOT volume data for each volunteer were linearly co-registered to account for subtle inter-scan motion using FLIRT (Jenkinson et al., 2002), part of FMRIB's Software Library (FSL, www.fmrib.ox.ac.uk/fsl (Smith et al., 2004)). Non-brain parenchyma signal was removed using an automated approach (Smith, 2002) with BET (part of FSL). Voxel-wise MWF maps were derived using mcDESPOT processing as previously outlined (Deoni, 2011).

2.3.2. Lesion and Tissue Type Identification—For the MS patients, MR visible lesions were marked on the proton density/T_2-*weighted* images by an experienced observer using a semi-automated lesion-mapping tool from the Jim software package (http://www.xinapse.com/home.php) local-thresholding technique, and manually corrected. White and grey matter masks were generated from the high-resolution volumetric T_1-*weighted* (MP-RAGE) image using the automated brain segmentation algorithm FAST (Zhang et al., 2001) (part of FSL) with a standard brain template, followed by in-plane erosion. For the MS patients, the lesion markings were co-registered with linear image registration (12 degrees of freedom) between the proton density-*weighted* image and the high-resolution volumetric T_1-*weighted* image, and subtracted from the WM and GM masks to obtain conservative normal-appearing WM (NAWM) and GM (NAGM) masks.

2.3.3. Native Space MWF Analysis—To align the mcDESPOT MWF results with the anatomical images for each individual, the high flip angle T_1-*weighted* mcDESPOT SPGR image was linearly co-registered (with 12 degrees of freedom) to the anatomical MP-RAGE image. The calculated transformation matrix was then applied to the individual's MWF map. The WM, GM and lesion masks were super-imposed on the aligned MWF map to obtain tissue-specific histograms. Histograms were calculated by summing the number of voxels with MWF values within 100 uniform bins between 0 and 30%. To account for differences in brain size and tissue volume, each individual's histogram was normalized with respect to the area of the histogram. The mean, variance and skewness of each tissue histogram, for each subject, were then determined. The histogram mean (or first moment) reflects the average value within the tissue type, and is expected to shift to lower values in areas of reduced myelin. The variance (or second moment) provides a measure of the variability of values and an increase could reflect increased heterogeneity in damaged tissue. The skewness (or third moment) measures the lopsidedness of the distribution; changes in skewness could reflect a shift in peak position or an increase in number of pixels with values to one side of the peak.

A Mann-Whitney test was used to assess between-group differences in MRI measures of global WM and GM damage. EDSS was correlated with MRI measures of global WM and GM damage using Spearman's rank order correlation coefficient. The coefficient of variation (CoV, standard deviation divided by the mean) was calculated to assess the reproducibility of the average MWF values within PPMS and control WM and GM, both across-subject as well as within-subject for those who were rescanned.

2.3.4. TBSS Analysis—A limitation of histogram analysis approaches is the omission of spatial location, potentially a key differentiating factor in clinical symptom and severity. To spatially compare MWF values across subjects and groups, we applied tract-based spatial statistics (TBSS) (Smith et al., 2006). Originally formulated for the analysis of DTI-derived fractional anisotropy (FA) maps, TBSS reduces biases due to inaccurate spatial registration by performing analysis along a skeletonized WM mask representing the mid-line of each WM pathway. As TBSS does not make use of DTI fibre orientation information, it may be directly applied to MWF maps with minor modification. Individual MWF images were nonlinearly aligned to every other using spline-based free-form deformation (using the standard TBSS registration methods), and the most representative MWF map was assigned as the target template. The target was then affine-aligned into MNI152 standard space, and each individual's MWF map was transformed to this space by combining the nonlinear transform to the target template with the affine transform to MNI152 space. The cross-subject mean MWF map was computed and used to generate a WM tract "skeleton", which was thresholded at MWF > 0.1 (determined through visual inspection of the skeleton to include the maximum amount of data with good cross-subject variability, as is done for FA TBSS). Individual MWF images were projected onto the skeleton for statistical comparison, restricting the analysis to the centers of WM tracts by searching for maximum MWF values perpendicular to the tract direction as is done for FA data as, similarly to FA, we expect (and observe) that MWF values decrease toward the edge of tracts due to increased partial volume with GM or CSF. Further, MWF doesn't suffer the confound of crossing fibres, where FA is reduced even in the centre of multiple WM tracts. However, in the event that MWF isn't anatomically at a maximum at the tract centre (for example, if MS targets a particular part of the tract in its earliest stages), the projection of maximum values provides a more conservative comparison.

The lesion masks were also transformed into MNI152 space. All points on the TBSS skeleton where one of the patients had a lesion were excluded from any analysis specific to NAWM. This process reduced the number of voxels in the skeleton from 81,831 to 74,853.

Group differences in MWF, and relationships between MWF and clinical measures were tested using Randomise (Nichols and Holmes, 2002) along the TBSS skeleton. Statistical significance was defined as $p < 0.05$, corrected for multiple comparisons by controlling family-wise error rate after Threshold-Free Cluster Enhancement (TFCE) (Smith and Nichols, 2009). Scan-rescan reproducibility of the MWF values along the TBSS WM skeleton was measured by creating the skeleton from the subset of data including only those subjects who were scanned twice, independently for each time point but following the identical procedure. The CoV was measured voxel-wise for each group (PPMS patients and controls).

2.3.5. Individual MWF Map Analysis—Whilst confirming group differences in MWF and associations between MWF and clinical symptoms are essential early steps towards establishing the efficacy of MWF as a biomarker in PPMS, identification of early tissue alteration in *individual* patients could have profound implications in treatment decisions and monitoring. One potential approach, borrowed from PET imaging, is to compare individual datasets with a matched normative template using Z-statistics. This approach highlights

areas of statistical difference in an individual from the population mean. The 3D nature of mcDESPOT makes this approach possible with MWF data for the first time.

To compare individual PPMS patient MWF maps to the healthy population, a normative 3D 'atlas' representing the MWF mean and standard deviation was created from a population of age-matched healthy controls. The healthy MWF maps were calculated, non-linearly aligned to the MNI standard space template (Collins et al., 1994) using a multi-scale approach, and averaged. To restrict our analysis to consistent anatomical voxels (those with a high correspondence between individuals, i.e., white and deep grey matter), voxels with a MWF CoV across subjects of greater than 75% were excluded (as determined through observation).

PPMS patient MWF maps were non-linearly aligned to the atlas (via registration to the MNI template) following lesion masking. Finally, for each voxel, a Z-score was calculated comparing the individual patient MWF values to the control group distribution. Voxels with $p < 0.05$ (corrected for multiple comparisons) were considered to be significantly reduced. For each patient, the number of significantly reduced voxels was summed over the whole brain to yield a measure of the volume of significantly decreased MWF.

3. RESULTS

3.1. Reproducibility

The average MWF in controls was found to be highly reproducible across volunteers and scans. Across the 17 healthy volunteers, the mean MWF CoV was 7.7% in WM and 19.5% in GM.

MWF scan-rescan difference, calculated from the 7 rescanned controls, was 0.9% (range 0.05-2.0%) in WM and 0.5% (range 0.06-1.1%) in GM. These results correspond to a within-subject scan-rescan CoV of 3.8% in WM and 7.9% in GM.

For PPMS patients, there was (as expected) more variability in MWF values across subjects, and slightly greater variation between scans for a single subject. Across all 17 PPMS patients, the mean MWF CoV was 11.1% in NAWM and 22.1% in normal appearing NAGM. For the 9 PPMS patients who underwent repeat MWF scans, and the average within patient rescan MWF difference measured between scan 1 and scan 2 was 1.2% (range 0.05-2.0%) in NAWM and 0.8% (range 0.6-1.5%) in NAGM, corresponding to a scan-rescan CoV of 4.7% in NAWM and 14.3% in NAGM.

On a voxel-wise basis, the scan-rescan CoV across the TBSS WM skeleton was generally between 3.5 and 6.5% for controls (median 5.0%, mode 3.4%). Once again, results were slightly more variable for PPMS patients with the CoV falling generally between 4.5% and 7.5% (median 5.8%, mode 4.4%). Spatially, no particular areas stand out as having a significantly higher CoV in either controls or PPMS patients, or differing between controls and patients (see Figure 1).

3.2. MWF Differences between Tissue Types

3.2.1. Global Analysis—Figure 2 shows the group mean MWF histograms for different tissue types for PPMS patients and controls.

These graphs clearly illustrate a significant reduction in global WM MWF between PPMS patients and controls (6%, p=0.04); greater patient MWF variance (23%, p=0.009); and reduced negative skew (28%, p=0.01) within patients. Examining GM, no significant

difference in mean MWF or variance was found, however, the distribution was more positively skewed for the PPMS group (14%, p=0.03).

While very heterogeneous, lesions had on average far lower MWF values than WM in both controls (61%, p<0.001) or patients (59%, p<0.001), but still more than GM in both groups. Lesions also had greater variance of MWF values than WM or GM (all p<0.001).

3.2.2. Regional Analysis—Results of our TBSS analysis are shown in Figure 3. Patients showed significantly reduced (p<0.05, fully corrected) MWF compared to controls throughout the bulk of the TBSS WM skeleton. Specific regions included the corticospinal tracts (predominantly on the left, in the corona radiata and WM adjacent to the motor cortex), the corpus callosum, thalamic radiation, optic radiation, fornix, superior and inferior longitudinal fasciculus, and cingulum.

3.3. Correlations Between MWF and Disability

From the global histogram analysis, significant correlations with EDSS were found with NAWM MWF variance (p = 0.05, R = 0.42), histogram skewness (p = 0.02, R = 0.49) and, most significantly, volume of significantly decreased MWF (p = 0.008, R = 0.58). Mean NAWM MWF had a trend to decrease with increasing EDSS (p = 0.08, R = −0.43). None of the GM metrics was correlated with EDSS (minimum p>0.3). Though not significant, a trend for EDSS to increase with lesion load was noted (p=0.06, R=0.47).

Along the TBSS WM skeleton, a significant *negative* correlation (p<0.05, corrected) was found between MWF and EDSS, as well as several FS scores in areas identified in red in Figure 4. The negative correlation reflected *reduced* myelin content predicting *increased* disability score, or more severe symptoms. In all cases, including age as a covariate did not alter the pattern of results but the loss in statistical power decreased the significance level slightly; while most results were still significant, some were reduced just below the significance threshold. It should be noted that age was not significantly correlated with MWF for this cohort at any point in the TBSS skeleton.

The significant relationship between MWF and EDSS was widespread throughout the brain, including the corpus callosum, and frontal, temporal, parietal and occipital WM (R = −0.53). The cerebellar score was also correlated with MWF through most of the WM tracts (R = −0.72), and while correlations were not significant in the cerebellum itself, trends (p<0.07, corrected, as shown in blue in Figure 4) were found in the left middle cerebellar peduncle and cerebral peduncle. The mental and sensory FS score correlations were more localized, with the mental score correlations (R = −0.58) found predominantly in anterior regions such as the frontal lobes and genu of the corpus callosum, and sensory score correlations (R = −0.74) in more posterior regions, closer to the sensory cortex. While the mental score correlations were bilateral, the significant correlations between MWF and the sensory FS score were found only on the left, although a few regions on the right (posterior corona radiate and thalamic radiation) were just below significance (p<0.07, corrected, as shown in blue in Figure 4).

No significant correlations were identified for the visual, brainstem, bladder, or pyramidal FS scores, nor disease duration.

3.4. Individual Patient Differences

Figure 5 displays example slices through the Z-score maps of 3 female PPMS patients of similar age (between 49 and 55).

Patient A had a small lesion load (1.6cm^3), low EDSS (1.5), and had very few regions of decreased MWF compared to the control atlas. Regions of significantly decreased MWF corresponded to lesions visible on the T_2-weighted image, but with a greater spatial extent than can be seen on the conventional image. Her MWF histogram was similar to that of healthy controls.

Patient B also had a small lesion load (1.4cm^3) but much higher EDSS (6.5). She showed reduced MWF diffusely throughout her WM, and displayed several areas of significantly reduced MWF, including the corpus callosum (visible in the sagittal Z-score map of Figure 4). Her MWF histogram showed a shift to lower MWF for the NAWM compared to controls.

Patient C had a large lesion load (7.1cm^3) and an EDSS of 5.5. She exhibited reduced MWF values globally throughout her white matter, beyond that of Patient B and her NAWM MWF histogram showed many more voxels at lower MWF values than in controls.

4. DISCUSSION

Calculated scan-rescan CoV values correspond well with other mcDESPOT studies of healthy controls (Dean and Deoni, 2011; Deoni et al., 2009), and are much smaller than for traditional multi-echo T_2-relaxation derived MWF values (Vavasour et al., 2006), indicating a potentially increased sensitivity for detecting subtle differences between indivicual patients as well as patient groups. For the TBSS results, the CoV values were consistent with TBSS results of FA as derived from DTI data in controls (Smith et al., 2006). The slightly higher scan-rescan variance found in the PPMS patients is expected given the globally reduced MWF values, greater heterogeneity of tissue and spread of MWF values, and the expected increased subject motion. However the measurement stability suggests mcDESPOT is well suited to longitudinal studies.

Globally, we observed a 6% reduction in mean MWF values in WM within the PPMS patients compared to healthy controls. This value is comparable, if not larger than, differences previously shown using MTR (between 1 and 3%) (Dehmeshki et al., 2003; Khaleeli et al., 2007; Vrenken et al., 2007), mean diffusivity (between 3 and 5%) (Ceccarelli et al., 2009; Rovaris et al., 2002; Vrenken et al., 2006b), or FA (between 5 and 6%) (Ceccarelli et al., 2009; Vrenken et al., 2006b). This result may suggest that MWF is equally, if not more, sensitive to disease-related tissue change and, combined with the proposed enhanced specificity of MWF over these other markers, supports the inclusion of MWF imaging to detect changes in PPMS NAWM.

As MWF may be derived using alternative approaches, it is useful, albeit challenging, to compare the global MWF reductions observed in this study using mcDESPOT to those using the more established multi-echo T_2 technique (MacKay et al., 1994). In the first account of MWF in MS, Laule et al (Laule et al., 2004) reported an average MWF reduction of 16% across five normal-appearing WM regions of interest in patients compared to controls. However, this work comprised a heterogeneous cohort of 33 MS patients (24 relapsing remitting, 8 secondary progressive, and only 1 PPMS), and relied on a single-slice imaging technique, which makes inter-subject registration and comparison difficult. Using a more volumetric 16-slice technique (Oh et al., 2006), Oh et al (Oh et al., 2007) reported a 9% reduction of mean NAWM MWF across a mixed cohort of 44 relapsing remitting and secondary progressive MS patients with a disease duration of greater than 5 years. This latter result is comparable to our results. The remaining difference may be due to the heterogeneous composition of the prior study populations, whereas we have included only PPMS patients. MTR and DTI studies have reported smaller NAWM changes in PPMS than

in either relapsing remitting or secondary progressive MS (Filippi et al., 2000; Tortorella et al., 2000; Vrenken et al., 2006a; Vrenken et al., 2006b; Vrenken et al., 2007).

Whilst a global reduction in MWF was observed in PPMS WM compared to controls, we did not observe similar significant differences within GM. However, a small but statistically significant decrease was noted in the positive skewness of PPMS GM histograms, suggesting a shift toward reduced MWF values for PPMS GM compared to control GM. Other imaging studies have shown differences in PPMS GM. These include reduced GM volume (Bodini et al., 2009), reduced MTR (Dehmeshki et al., 2003) and increased mean diffusivity (Ceccarelli et al., 2009; Rovaris et al., 2002; Vrenken et al., 2006b). The relatively small measured change in GM MWF in PPMS could be methodological; MWF values are much lower and more variable in GM than in WM, making subtle changes more difficult to detect. Further, our conservative sampling of GM eroded away from partial volume boundaries may miss regions more prone to demyelination. More speculatively, our results could imply that demyelination is not the sole cause of previously reported GM differences in imaging metrics, as those measures can also be affected by inflammation or axonal loss.

Using TBSS to provide spatial specificity, we found reduced MWF in the PPMS patients compared to controls diffusely throughout core WM. The tracts showing significantly reduced MWF values match those previously shown to have reduced FA in PPMS (Bodini et al., 2009). Whilst we would not expect all patients to suffer demyelination in the same regions, or be at the same stage of demyelination, this result shows that no single brain region is driving the MWF difference observed in the histogram analysis, nor the correlations noted between global measures of MWF and EDSS.

Few other studies have found correlations between whole-brain MR-measures and EDSS in PPMS (Dehmeshki et al., 2003; Rocca et al., 2011). Using the TBSS skeleton allowed us to investigate which brain regions were driving this correlation, as well as the more specific FS scores that make up the overall EDSS score. Significant correlations between MWF and EDSS were widespread; the lack of regional specificity is unsurprising as EDSS is an overall disability score. The significant correlations between MWF and the cerebellar FS score were also disseminated throughout the brain, with the surprising exception of the cerebellum itself, although correlations just below significance were found within the cerebellum. Of interest, the cerebellar FS score was the only FS score to be significantly correlated with EDSS, which may explain the more diffuse nature of these results. Encouragingly, the mental and sensory FS score correlations with MWF were found in clinically relevant locations, with the mental score being associated with reduced MWF in frontal white matter and the corpus callosum, and the sensory score apparently being affected primarily by posterior MWF losses, serving the sensory cortex. Only the correlations between MWF and the sensory score appeared to be unilateral, with stronger correlations on the patient left side, although a few regions on the right were just below significance. The lack of significant correlation between MWF and the visual score is likely due to the spatial resolution of the whole-brain study being inadequate to specifically isolate the optic nerve, while the pyramidal score is more likely to be more affected by the spinal cord, which was not imaged in this study.

Regional correlations between clinical disability and FA have been demonstrated using TBSS in relapsing remitting MS (Dineen et al., 2009; Giorgio et al., 2010), and PPMS (Bodini et al., 2009), and between clinical disability and higher probability of lesion in PPMS (Bodini et al., 2011). The greater spatial extent of correlations between EDSS and reduced MWF found in this study could indicate greater sensitivity to changes relevant to disability. The complementary and possibly more specific information afforded by multi-

component relaxation imaging may improve our understanding of the pathological processes driving clinical disability and progression.

The correlation between MWF and EDSS reported here indicates that MWF reflects changes in pathology relevant to disease expression. Further, the overlap of identified brain regions that show significant correlation between MWF and specific clinical FS scores with areas known to be involved in these functions supports the clinical relevance of MWF measures. However, these relationships are observed on a *group-level*, and are not particularly informative for the individual patient. Comparing individual patient MWF maps to a normative atlas provides immediate visual feedback of abnormalities throughout not only lesional tissue but also normal appearing brain tissue. This quantitative measurement is equally applicable at other field strengths, across centres, system manufacturers, and over time, providing a robust method for assessing patients consistently.

A potential limitation of this study is the omission of the spinal cord, which is known to be largely involved in PPMS. It is likely that assessing MWF throughout the spinal cord, in addition to the brain, will greatly increase the power to explain clinical symptoms. We have recently demonstrated the feasibility and application of mcDESPOT within healthy spinal cord (Kolind and Deoni, 2011), and future work will extend this to spinal cord in PPMS.

Another limitation of this study is the small sample size; while we were able to demonstrate significant group differences and correlations with disability, results should be interpreted with caution.

There are also limitations to mcDESPOT; while it does provide high-resolution full-brain coverage in feasible times, it is currently limited to examining two water pools: the fast-relaxing myelin water pool and more slowly-relaxing intra- and extra-cellular water pool. Studies using more traditional multi-component relaxation techniques that allow fitting of a T_2 distribution can detect additional water pools, and long-T_2 components have been demonstrated in MS lesion and normal appearing white matter (Laule et al., 2006b). mcDESPOT also yields higher MWF values than are generally observed using multi-echo T_2-relaxation, which could be the result of the two-pool model of mcDESPOT, magnetization transfer effects, or differences in modeling of exchange between pools; further study is required (Deoni, 2011; Kolind and Deoni, 2011). Results reported herein illustrate the ability of MWF to explain current symptoms. Perhaps more important will be the investigation of whether MWF reflects clinical changes over time, through longitudinal studies. The atlas-based approach introduced in this work provides the potential for such analysis, tracking changes in Z-score values throughout an individual's brain over time. Such analysis has latent potential for disease monitoring and the evaluation of putative treatments. The clinical relevance of mcDESPOT-derived MWF values in this study support the inclusion of mcDESPOT in future MS studies.

Acknowledgments

Sincere thanks to our volunteers and their families, and to the radiographers (particularly Steven Knight and Stuart Wilson) and staff at the Oxford Centre for Clinical Magnetic Resonance Research.

FUNDING This work was supported by the Multiple Sclerosis Society of Canada [to S.K.]; the University of Oxford John Fell OUP Research Fund [092/305 to S.K. and L.M.]; the Medical Research Council [G0901996 to L.M.]; the Wellcome Trust [WT090955AIA to H.J.B.]; and the Oxford NIHR Biomedical Research Centre.

REFERENCES

Beaulieu C. The basis of anisotropic water diffusion in the nervous system - a technical review. NMR in Biomedicine. 2002; 15:435–455. [PubMed: 12489094]

Bitsch A, Schuchardt J, Bunkowski S, Kuhlmann T, Bruck W. Acute axonal injury in multiple sclerosis. Correlation with demyelination and inflammation. Brain. 2000; 123(Pt 6):1174–1183. [PubMed: 10825356]

Bodini B, Battaglini M, De Stefano N, Khaleeli Z, Barkhof F, Chard D, Filippi M, Montalban X, Polman C, Rovaris M, Rovira A, Samson R, Miller D, Thompson A, Ciccarelli O. T2 lesion location really matters: a 10 year follow-up study in primary progressive multiple sclerosis. J Neurol Neurosurg Psychiatry. 2011; 82:72–77. [PubMed: 20627965]

Bodini B, Khaleeli Z, Cercignani M, Miller DH, Thompson AJ, Ciccarelli O. Exploring the relationship between white matter and gray matter damage in early primary progressive multiple sclerosis: an in vivo study with TBSS and VBM. Hum Brain Mapp. 2009; 30:2852–2861. [PubMed: 19172648]

Ceccarelli A, Rocca MA, Valsasina P, Rodegher M, Pagani E, Falini A, Comi G, Filippi M. A multiparametric evaluation of regional brain damage in patients with primary progressive multiple sclerosis. Hum Brain Mapp. 2009; 30:3009–3019. [PubMed: 19172642]

Collins DL, Neelin P, Peters TM, Evans AC. Automatic 3D intersubject registration of MR volumetric data in standardized Talairach space. J Comput Assist Tomogr. 1994; 18:192–205. [PubMed: 8126267]

Dean, DC.; Deoni, SCL. Reproducibility of Myelin Water Fraction Maps Using mcDESPOT. ISMRM White Matter Study Group International Workshop on Advanced White Matter Imaging; Reykjavik, Iceland. 2011. p. P9

Dehmeshki J, Chard DT, Leary SM, Watt HC, Silver NC, Tofts PS, Thompson AJ, Miller DH. The normal appearing grey matter in primary progressive multiple sclerosis: a magnetisation transfer imaging study. J Neurol. 2003; 250:67–74. [PubMed: 12527995]

Deoni SC. Correction of main and transmit magnetic field (B(0) and B(1)) inhomogeneity effects in multicomponent-driven equilibrium single-pulse observation of T(1) and T(2). Magn Reson Med. 2011; 65:1021–1035. [PubMed: 21413066]

Deoni SC, Rutt BK, Arun T, Pierpaoli C, Jones DK. Gleaning multicomponent T1 and T2 information from steady-state imaging data. Magn Reson Med. 2008; 60:1372–1387. [PubMed: 19025904]

Deoni, SC.; Samson, R.; Wheeler-Kingshot, CA. Intra and Inter-Site Reproducibility of Myelin Water Volume Fraction Values Derived using mcDESPOT. 17th Annual Meeting of the International Society of Magnetic Resonance in Medicine; Honolulu, USA. 2009. p. 4530

Dineen RA, Vilisaar J, Hlinka J, Bradshaw CM, Morgan PS, Constantinescu CS, Auer DP. Disconnection as a mechanism for cognitive dysfunction in multiple sclerosis. Brain. 2009; 132:239–249. [PubMed: 18953055]

Filippi M, Inglese M, Rovaris M, Sormani MP, Horsfield P, Iannucci PG, Colombo B, Comi G. Magnetization transfer imaging to monitor the evolution of MS: a 1-year follow-up study. Neurology. 2000; 55:940–946. [PubMed: 11061248]

Gareau PJ, Rutt BK, Karlik SJ, Mitchell JR. Magnetization transfer and multicomponent T2 relaxation measurements with histopathologic correlation in an experimental model of MS. Journal of Magnetic Resonance Imaging. 2000; 11:586–595. [PubMed: 10862056]

Giorgio A, Palace J, Johansen-Berg H, Smith SM, Ropele S, Fuchs S, Wallner-Blazek M, Enzinger C, Fazekas F. Relationships of brain white matter microstructure with clinical and MR measures in relapsing-remitting multiple sclerosis. J Magn Reson Imaging. 2010; 31:309–316. [PubMed: 20099343]

Grenier D, Pelletier D, Normandeau M, Newitt D, Nelson S, Goodkin DE, Majumdar S. T2 relaxation time histograms in multiple sclerosis. Magn Reson Imaging. 2002; 20:733–741. [PubMed: 12591569]

Harsan LA, Poulet P, Guignard B, Steibel J, Parizel N, de Sousa PL, Boehm N, Grucker D, Ghandour MS. Brain dysmyelination and recovery assessment by noninvasive in vivo diffusion tensor magnetic resonance imaging. J Neurosci Res. 2006; 83:392–402. [PubMed: 16397901]

Jenkinson M, Bannister P, Brady M, Smith S. Improved optimization for the robust and accurate linear registration and motion correction of brain images. Neuroimage. 2002; 17:825–841. [PubMed: 12377157]

Khaleeli Z, Sastre-Garriga J, Ciccarelli O, Miller DH, Thompson AJ. Magnetisation transfer ratio in the normal appearing white matter predicts progression of disability over 1 year in early primary progressive multiple sclerosis. J Neurol Neurosurg Psychiatry. 2007; 78:1076–1082. [PubMed: 17287235]

Kolind SH, Deoni SC. Rapid three-dimensional multicomponent relaxation imaging of the cervical spinal cord. Magn Reson Med. 2011; 65:551–556. [PubMed: 20882672]

Kolind SH, Laule C, Vavasour IM, Li DK, Traboulsee AL, Mädler B, Moore GR, Mackay AL. Complementary information from multi-exponential T(2) relaxation and diffusion tensor imaging reveals differences between multiple sclerosis lesions. Neuroimage. 2008; 40:77–85. [PubMed: 18226549]

Kozlowski P, Raj D, Liu J, Lam C, Yung AC, Tetzlaff W. Characterizing white matter damage in rat spinal cord with quantitative MRI and histology. J Neurotrauma. 2008; 25:653–676. [PubMed: 18578635]

Kurtzke JF. Rating neurologic impairment in multiple sclerosis: an expanded disability status scale (EDSS). Neurology. 1983; 33:1444–1452. [PubMed: 6685237]

Kutzelnigg A, Lucchinetti CF, Stadelmann C, Bruck W, Rauschka H, Bergmann M, Schmidbauer M, Parisi JE, Lassmann H. Cortical demyelination and diffuse white matter injury in multiple sclerosis. Brain. 2005; 128:2705–2712. [PubMed: 16230320]

Laule C, Kozlowski P, Leung E, Li DKB, MacKay AL, Moore GRW. Myelin water imaging of multiple sclerosis at 7 T: Correlations with histopathology. Neuroimage. 2008; 40:1575–1580. [PubMed: 18321730]

Laule C, Leung E, Li DK, Traboulsee AL, Paty DW, MacKay AL, Moore GR. Myelin water imaging in multiple sclerosis: quantitative correlations with histopathology. Mult Scler. 2006a; 12:747–753. [PubMed: 17263002]

Laule, C.; Vavasour, IM.; Kolind, SH.; Traboulsee, AL.; Li, DKB.; MacKay, AL. Long-T2 Imaging: Evidence of a New Water Reservoir in Multiple Sclerosis. 14th Annual Meeting of the International Society of Magnetic Resonance in Medicine; Seattle, USA. 2006b. p. 446

Laule C, Vavasour IM, Kolind SH, Traboulsee AL, Moore GRW, Li DKB, MacKay AL. Long T2 Water in Multiple Sclerosis: What else can we learn from multi-echo T2 Relaxation? Journal of Neurology. 2007; 254:1579–1587. [PubMed: 17762945]

Laule C, Vavasour IM, Leung E, Li DK, Kozlowski P, Traboulsee AL, Oger J, Mackay AL, Moore GR. Pathological basis of diffusely abnormal white matter: insights from magnetic resonance imaging and histology. Mult Scler. 2011; 17:144–150. [PubMed: 20965961]

Laule C, Vavasour IM, Moore GRW, Oger J, Li DKB, Paty DW, MacKay AL. Water content and myelin water fraction in multiple sclerosis: A T2 relaxation study. Journal of Neurology. 2004; 251:284–293. [PubMed: 15015007]

MacKay A, Whittall K, Adler J, Li D, Paty D, Graeb D. In vivo visualization of myelin water in brain by magnetic resonance. Magn Reson Med. 1994; 31:673–677. [PubMed: 8057820]

Manfredonia F, Ciccarelli O, Khaleeli Z, Tozer DJ, Sastre-Garriga J, Miller DH, Thompson AJ. Normal-appearing brain t1 relaxation time predicts disability in early primary progressive multiple sclerosis. Arch Neurol. 2007; 64:411–415. [PubMed: 17353385]

Miller DH, Leary SM. Primary-progressive multiple sclerosis. Lancet Neurol. 2007; 6:903–912. [PubMed: 17884680]

Miller DH, Thompson AJ, Filippi M. Magnetic resonance studies of abnormalities in the normal appearing white matter and grey matter in multiple sclerosis. J Neurol. 2003; 250:1407–1419. [PubMed: 14673572]

Moore GRW, Leung E, MacKay AL, Vavasour IM, Whittall KP, Cover KS, Li DK, Hashimoto SA, Oger J, Sprinkle TJ, Paty DW. A pathology-MRI study of the short-T2 component in formalin-fixed multiple sclerosis brain. Neurology. 2000; 55:1506–1510. [PubMed: 11094105]

Nichols TE, Holmes AP. Nonparametric permutation tests for functional neuroimaging: a primer with examples. Hum Brain Mapp. 2002; 15:1–25. [PubMed: 11747097]

Odrobina EE, Lam TY, Pun T, Midha R, Stanisz GJ. MR properties of excised neural tissue following experimentally induced demyelination. NMR Biomed. 2005; 18:277–284. [PubMed: 15948233]

Oh J, Han ET, Lee MC, Nelson SJ, Pelletier D. Multislice brain myelin water fractions at 3T in multiple sclerosis. J Neuroimaging. 2007; 17:156–163. [PubMed: 17441837]

Oh J, Han ET, Pelletier D, Nelson SJ. Measurement of in vivo multi-component T2 relaxation times for brain tissue using multi-slice T2 prep at 1.5 and 3 T. Magn Reson Imaging. 2006; 24:33–43. [PubMed: 16410176]

Patrikios P, Stadelmann C, Kutzelnigg A, Rauschka H, Schmidbauer M, Laursen H, Sorensen PS, Bruck W, Lucchinetti C, Lassmann H. Remyelination is extensive in a subset of multiple sclerosis patients. Brain. 2006; 129:3165–3172. [PubMed: 16921173]

Polman CH, Reingold SC, Edan G, Filippi M, Hartung HP, Kappos L, Lublin FD, Metz LM, McFarland HF, O'Connor PW, Sandberg-Wollheim M, Thompson AJ, Weinshenker BG, Wolinsky JS. Diagnostic criteria for multiple sclerosis: 2005 revisions to the "McDonald Criteria". Ann Neurol. 2005; 58:840–846. [PubMed: 16283615]

Pun TW, Odrobina E, Xu QG, Lam TY, Munro CA, Midha R, Stanisz GJ. Histological and magnetic resonance analysis of sciatic nerves in the tellurium model of neuropathy. Journal of the Peripheral Nervous System. 2005; 10:38–46. [PubMed: 15703017]

Rabe-Jabloska J. [Significance of synaptic connectivity reduction for pathogenesis, clinical picture and course of schizophrenia]. Psychiatria Polska. 2003; 37:951–964. [PubMed: 14727368]

Revesz T, Kidd D, Thompson AJ, Barnard RO, McDonald WI. A comparison of the pathology of primary and secondary progressive multiple sclerosis. Brain. 1994; 117(Pt 4):759–765. [PubMed: 7922463]

Rocca MA, Absinta M, Filippi M. The role of advanced magnetic resonance imaging techniques in primary progressive MS. J Neurol. 2011

Rovaris M, Bozzali M, Iannucci G, Ghezzi A, Caputo D, Montanari E, Bertolotto A, Bergamaschi R, Capra R, Mancardi GL, Martinelli V, Comi G, Filippi M. Assessment of normal-appearing white and gray matter in patients with primary progressive multiple sclerosis: a diffusion-tensor magnetic resonance imaging study. Arch Neurol. 2002; 59:1406–1412. [PubMed: 12223026]

Rovaris M, Judica E, Gallo A, Benedetti B, Sormani MP, Caputo D, Ghezzi A, Montanari E, Bertolotto A, Mancardi G, Bergamaschi R, Martinelli V, Comi G, Filippi M. Grey matter damage predicts the evolution of primary progressive multiple sclerosis at 5 years. Brain. 2006; 129:2628–2634. [PubMed: 16921179]

Sastre-Garriga J, Ingle GT, Chard DT, Cercignani M, Ramio-Torrenta L, Miller DH, Thompson AJ. Grey and white matter volume changes in early primary progressive multiple sclerosis: a longitudinal study. Brain. 2005a; 128:1454–1460. [PubMed: 15817511]

Sastre-Garriga J, Ingle GT, Chard DT, Ramio-Torrenta L, McLean MA, Miller DH, Thompson AJ. Metabolite changes in normal-appearing gray and white matter are linked with disability in early primary progressive multiple sclerosis. Arch Neurol. 2005b; 62:569–573. [PubMed: 15824254]

Schmierer K, Altmann DR, Kassim N, Kitzler H, Kerskens CM, Doege CA, Aktas O, Lunemann JD, Miller DH, Zipp F, Villringer A. Progressive change in primary progressive multiple sclerosis normal-appearing white matter: a serial diffusion magnetic resonance imaging study. Mult Scler. 2004; 10:182–187. [PubMed: 15124765]

Smith SM. Fast robust automated brain extraction. Hum Brain Mapp. 2002; 17:143–155. [PubMed: 12391568]

Smith SM, Jenkinson M, Johansen-Berg H, Rueckert D, Nichols TE, Mackay CE, Watkins KE, Ciccarelli O, Cader MZ, Matthews PM, Behrens TE. Tract-based spatial statistics: voxelwise analysis of multi-subject diffusion data. Neuroimage. 2006; 31:1487–1505. [PubMed: 16624579]

Smith SM, Jenkinson M, Woolrich MW, Beckmann CF, Behrens TEJ, Johansen-Berg H, Bannister PR, De Luca M, Drobnjak I, Flitney DE. Advances in functional and structural MR image analysis and implementation as FSL. Neuroimage. 2004; 23:S208–S219. [PubMed: 15501092]

Smith SM, Nichols TE. Threshold-free cluster enhancement: addressing problems of smoothing, threshold dependence and localisation in cluster inference. Neuroimage. 2009; 44:83–98. [PubMed: 18501637]

Stanisz GJ, Webb S, Munro CA, Pun T, Midha R. MR properties of excised neural tissue following experimentally induced neuroinflammation. Magnetic resonance in medicine. 2004; 51:473–479. [PubMed: 15004787]

Stewart WA, MacKay AL, Whittall KP, Moore GR, Paty DW. Spin-spin relaxation in experimental allergic encephalomyelitis. Analysis of CPMG data using a non-linear least squares method and linear inverse theory. Magnetic Resonance in Medicine. 1993; 29:767–775. [PubMed: 8350719]

Tortorella C, Viti B, Bozzali M, Sormani MP, Rizzo G, Gilardi MF, Comi G, Filippi M. A magnetization transfer histogram study of normal-appearing brain tissue in MS. Neurology. 2000; 54:186–193. [PubMed: 10636146]

Vavasour IM, Clark CM, Li DK, Mackay AL. Reproducibility and reliability of MR measurements in white matter: clinical implications. Neuroimage. 2006; 32:637–642. Epub 2006 May 2003. [PubMed: 16677833]

Vavasour, IM.; Laule, C.; Kolind, SH.; Li, DKB.; Traboulsee, AL.; MacKay, AL. Using relaxation, magnetization transfer and diffusion to characterise multiple sclerosis lesion pathology. 15th Annual Meeting of the International Society of Magnetic Resonance in Medicine; Berlin, Germany. 2007. p. 272

Vavasour IM, Laule C, Li DK, Traboulsee AL, MacKay AL. Is the magnetization transfer ratio a marker for myelin in multiple sclerosis? J Magn Reson Imaging. 2011; 33:713–718. [PubMed: 21563257]

Vavasour IM, Whittall KP, MacKay AL, Li DK, Vorobeychik G, Paty DW. A comparison between magnetization transfer ratios and myelin water percentages in normals and multiple sclerosis patients. Magnetic Resonance in Medicine. 1998; 40:763–768. [PubMed: 9797161]

Vrenken H, Geurts JJ, Knol DL, van Dijk, L N, Dattola V, Jasperse B, van Schijndel RA, Polman CH, Castelijns JA, Barkhof F, Pouwels PJ. Whole-brain T1 mapping in multiple sclerosis: global changes of normal-appearing gray and white matter. Radiology. 2006a; 240:811–820. [PubMed: 16868279]

Vrenken H, Pouwels PJ, Geurts JJ, Knol DL, Polman CH, Barkhof F, Castelijns JA. Altered diffusion tensor in multiple sclerosis normal-appearing brain tissue: cortical diffusion changes seem related to clinical deterioration. J Magn Reson Imaging. 2006b; 23:628–636. [PubMed: 16565955]

Vrenken H, Pouwels PJ, Ropele S, Knol DL, Geurts JJ, Polman CH, Barkhof F, Castelijns JA. Magnetization transfer ratio measurement in multiple sclerosis normal-appearing brain tissue: limited differences with controls but relationships with clinical and MR measures of disease. Mult Scler. 2007; 13:708–716. [PubMed: 17613597]

Webb S, Munro CA, Midha R, Stanisz GJ. Is multicomponent T2 a good measure of myelin content in peripheral nerve? Magn Reson Med. 2003; 49:638–645. [PubMed: 12652534]

Zhang Y, Brady M, Smith S. Segmentation of brain MR images through a hidden Markov random field model and the expectation-maximization algorithm. Medical Imaging, IEEE Transactions on. 2001; 20:45–57.

Europe PMC Funders Author Manuscripts

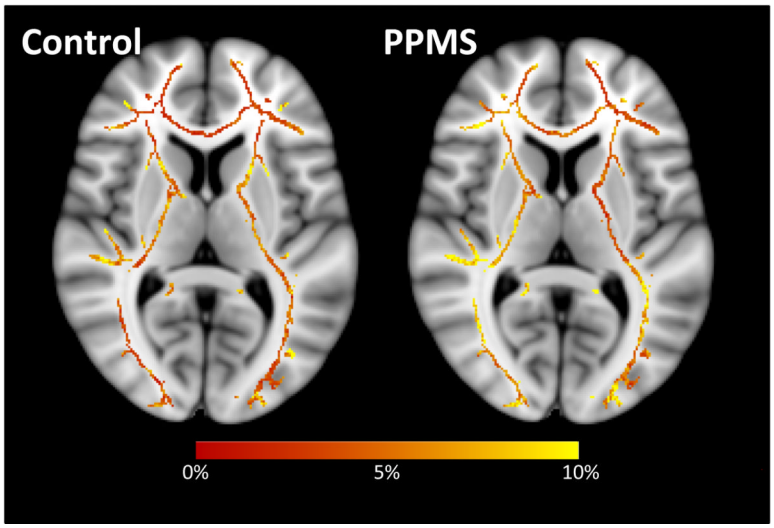

Figure 1.
Coefficient of variation along the MWF TBSS skeleton for the 7 healthy controls (left) and 9 PPMS patients (right) who underwent two MRI examinations.

Europe PMC Funders Author Manuscripts

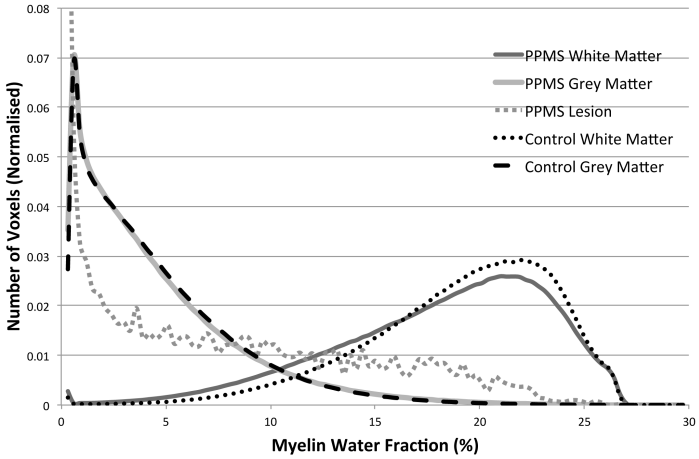

Figure 2.

Group mean MWF histograms of NAWM and NAGM and lesion (grey) in PPMS patients, and WM and GM (black) in controls. Changes to NAWM were significant compared to control WM in terms of mean, variance and skewness, while the skewness was significantly different in NAGM compared to control GM. Note that the vertical scale is limited for visibility of detail; the lesion MWF histogram reached 0.13 for MWF values between 0 and 0.3%.

Europe PMC Funders Author Manuscripts

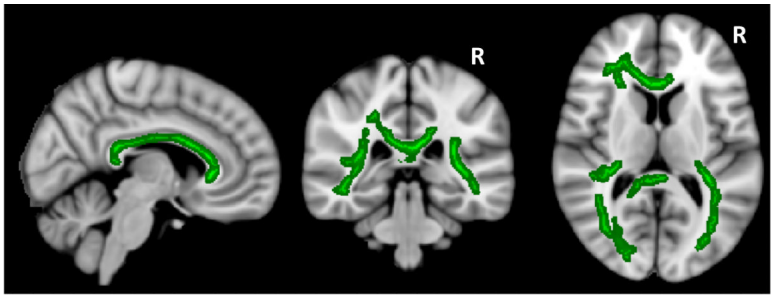

Figure 3.
Significant decreases in MWF (in green) for PPMS patients compared to healthy control WM ($p<0.05$, corrected).

Europe PMC Funders Author Manuscripts

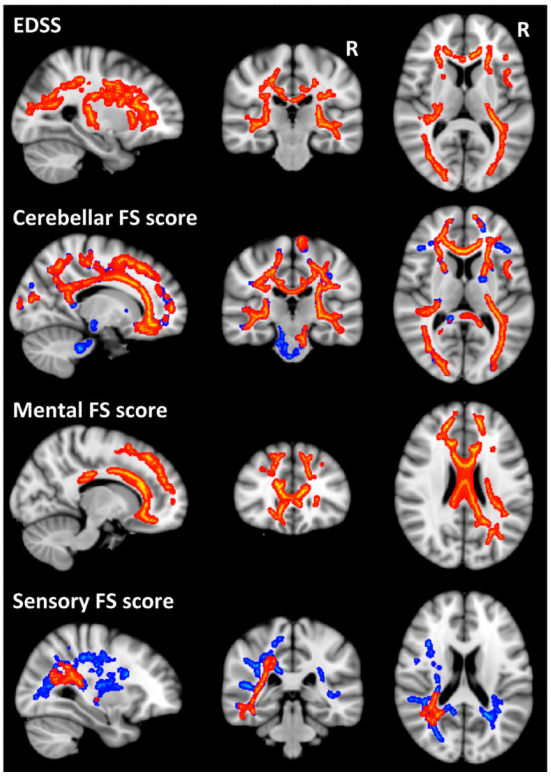

Figure 4.
Significant correlations between worsening clinical scores and decreased MWF values in red ($p<0.05$, corrected) with trends in blue ($p<0.07$, corrected).

Europe PMC Funders Author Manuscripts

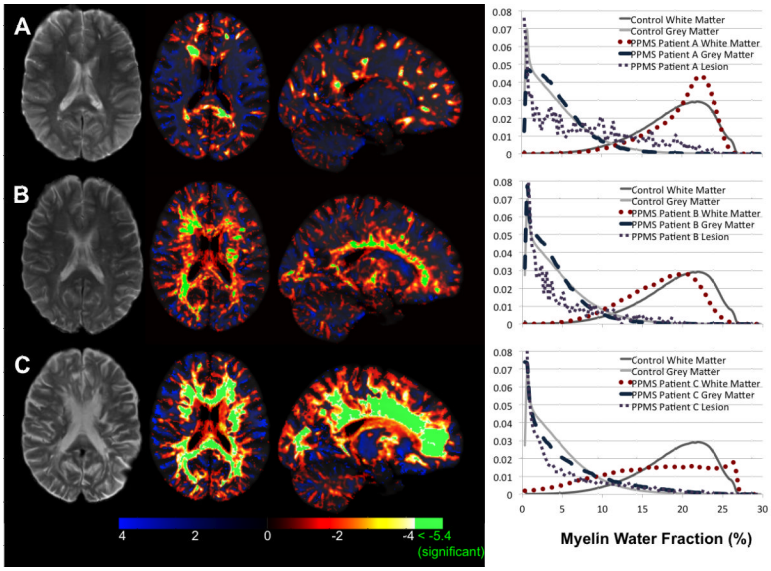

Figure 5.

T_2-weighted image (left), axial and sagittal Z-score map of MWF values compared to the group of matched healthy controls (middle) and histogram of MWF values (right) for three PPMS patients. PPMS Patient A had an EDSS of 1.5, Patient B had an EDSS of 6.5 and Patient C had an EDSS of 5.5.

Europe PMC Funders Author Manuscripts